Theriogenology 119 (2018) 183–188

Contents lists available at ScienceDirect

Theriogenology

journal homepage: www.theriojournal.com

An optimized controlled rate slow cooling protocol for bovine ovarian tissue cryopreservation by means of X-ray computed tomography

Ariadna Corral [a], Marcin Balcerzyk [a], Miguel Gallardo [b], Christiani A. Amorim [c], Ángel Parrado-Gallego [a], Ramón Risco [a, d, *]

[a] Centro Nacional de Aceleradores (Universidad de Sevilla-CSIC-Junta de Andalucía), Calle Thomas Alva Edison 7, 41092, Sevilla, Spain
[b] Ginemed Clínicas Sevilla, Calle Farmaceutico Murillo Herrera 3, 41010, Sevilla, Spain
[c] Pôle de Recherche en Gynécologie, Institut de Recherche Expérimentale et Clinique, Université Catholique de Louvain, Avenue Mounier 52, Bte. B1.52.02, 1200, Brussels, Belgium
[d] Departamento de Física Aplicada III, Escuela Técnica Superior de Ingeniería, Universidad de Sevilla, Camino Descubrimientos S/N, Isla Cartuja, 41092, Sevilla, Spain

ARTICLE INFO

Article history:
Received 13 April 2018
Received in revised form
27 June 2018
Accepted 29 June 2018
Available online 3 July 2018

Keywords:
CT imaging
Fertility preservation
Cryoprotectant visualization
Tissue permeation

ABSTRACT

Cryopreservation and subsequent transplantation of ovarian tissue is the only option to preserve fertility in certain patients facing gonadotoxic treatment. So far, cryopreservation of ovarian tissue has been carried out mostly by a controlled rate slow cooling process, typically known as *slow freezing*. Even though there are still some concerns about the iatrogenic damage on the follicle population, this technique has been used in the more than 100 live births reported to date. It is well known that the control of the cryoprotectant loading in the tissue is crucial to in a cryopreservation procedure. We have used the technology of X-ray computed tomography to assess the concentration and distribution of dimethyl sulfoxide (one of the cryoprotectants most used in fertility preservation) inside pieces of bovine ovarian tissue after its cryopreservation. The low voltage used in our device (75 kV) and the high electronic density of this cryoprotectant makes the X-ray attenuation proportional to its concentration. By assessing and comparing the permeation and homogeneity of the cryoprotectant inside ovarian tissue fragments subjected to a controlled rate slow cooling process, we have characterized the effect of variations in the main parameters involved in the process, with the goal of achieving an optimized protocol with higher permeation of the cryoprotectant in the tissue. The most promissory results were obtained by increasing the initial concentration of dimethyl sulfoxide in the vehicle solution from 10 to 20 % *v*/*v*.

1. Introduction

Cryopreservation of ovarian tissue is the only option of fertility preservation for certain cancer patients, such as pre-pubertal girls, for whom being subjected to a hormonal stimulation cycle for oocyte preservation is not possible [1]. Advantages of ovarian tissue cryopreservation are the high tolerance of the follicle population to freezing and thawing, and the possibility for immediate surgical collection of the tissue, done at any time of the women's cycle [1].

The most widely employed and successful method of ovarian tissue cryopreservation for fertility preservation is a controlled rate cooling slow cooling, known as *slow freezing* [1–5], with more than 100 cases of live births after transplantation reported [6,7]. Despite this promising data, current *slow freezing* protocols are empirical adaptations from the ones used for oocyte and embryo cryopreservation [5]. As a result, when this cooling process is employed in ovarian tissue, a more complex and dense biological system, it can damage the follicle population and the ovarian stroma. This iatrogenic damage can affect the viability of the tissue after transplantation [8,9].

The aim of this study was to optimize a conventional controlled rate slow cooling protocol for human ovarian tissue, focusing on achieving a more homogeneous distribution of the cryoprotectant (CPA) inside the tissue fragments during the cryopreservation procedure. For that purpose, we carried out a series of experiments with bovine ovarian tissue varying the following parameters of the controlled rate slow cooling protocol: the volume of the initial

* Corresponding author. Departamento de Física Aplicada III, Escuela Técnica Superior de Ingeniería, Universidad de Sevilla, Camino Descubrimientos s/n, Isla Cartuja, 41092, Sevilla, Spain. Tel.: +34 636211991.
E-mail address: ramon@us.es (R. Risco).

https://doi.org/10.1016/j.theriogenology.2018.06.031
0093-691X/

solution, the cooling rate (CR) from the seeding point to −40 °C, the initial Me_2SO concentration and the temperature and time of incubation of the initial solution. The control of the cryoprotectants penetration in tissues is crucial for avoiding both ice formation and toxicity damage in tissues [10]. Several methods of measurements of cryoprotectant permeation in tissues haven been attempted so far: differences on density [11,12], electric impedance [13,14] or refractive index [15]. Imaging methods (mostly nuclear magnetic resonance) have also been applied to monitor the cryoprotectants concentration inside tissues [16–19]. Herein we used an imaging technique based on X-ray computed tomography in order to assess the equilibration of the CPA inside the tissue, previously developed by our group [20]. The low energies used in our device (75 keV) makes it an excellent way to visualize and quantify the concentration of dimethyl sulfoxide (Me_2SO), one of the most used CPAs in the field of fertility preservation, thanks to the high electronic density of this molecule due to its sulfur atom [20].

2. Materials and methods

2.1. Experimental design

To optimize the freezing protocol for human ovarian tissue, we used bovine ovaries, due to their similarities with human ovaries in follicle size and growth pattern and stroma composition [21]. A total of 6 ovaries were cut into strips, cryopreserved using different freezing protocols and then analyzed by X-ray computed tomography to calculate the cryoprotectant concentrations in the fragments.

2.2. Collection of ovarian tissue

Ovaries were obtained from one-year-old heifers (n = 6), sacrificed in a local slaughterhouse (Matadero del Sur, Sevilla, Spain). They were transported to our laboratory in a saline solution at 37 °C and processed within the following 3 h. The ovaries were cut in a half and the medulla was removed. The cortex was then cut in 5x5x2-3 mm^3 strips (supplementary material, Table S1).

2.3. Freezing-thawing protocol

2.3.1. Control protocol

Freezing of bovine ovarian tissue samples was performed using a variation of Dolmans et al. protocol [22]. Briefly, one fragment was introduced in a cryovial (Nalgene, USA) containing 1.8 mL of the freezing solution (minimal essential medium + GlutamaxTM (MEM; Gibco, Invitrogen, Belgium) supplemented with 10 % v/v Me_2SO (Sigma Aldrich, Spain)). The cryovial was then placed in the freezing machine (Bio-Cool IV, model BCIV40D; FTS Systems, USA) at 0 °C and held for 15 min. The sample was subsequently cooled to −5.5 °C at 2 °C/min and held for another 15 min. The ice seeding was performed by touching the side of the cryovials at the height of the vehicle solution with some previously cooled forceps, until growth of ice crystals was observed. Ice was allowed to grow for another 15 min inside the ethanol bath. Afterwards, the cryovial was cooled down to −40 °C at 0.3 °C/min. The fast cooling (20 °C/min) until −150 °C was performed by exposing the cryovial to liquid nitrogen vapors, at 2 cm of height. The sample was finally quenched and stored in the liquid nitrogen tank. This protocol was considered as the control protocol for the optimization process.

2.3.2. Experimental variations

Table 1 shows the six different protocols we created by varying the four parameters that can influence ice formation and consequently cell survival: the volume of the cryoprotectant solution, the cooling rate, the initial cryoprotectant concentration, and the temperature and time of the tissue incubation. The total volume of the vehicle Me_2SO solution was studied and two volumes compared (1.8 mL and 0.8 mL). We also varied the cooling rate from the temperature of the seeding until −40 °C. This cooling rate (CR) controls the process of the controlled rate slow cooling: the rate of the extracellular ice formation and the CPA permeation and dehydration of the tissue. The control group uses a CR of 0.3 °C/min; variations tested were 0.1 °C/min and 1 °C/min. In addition, the initial CPA concentration used in the solution is also a limiting factor for the concentration achieved in the tissue at the end of the controlled rate slow cooling process. The initial concentration of the control group was 10 % v/v Me_2SO. We compared the effect on the tissue permeation of a lower concentration of 5 % v/v Me_2SO, and a higher concentration of 20 % v/v Me_2SO. It is important to highlight that the seeding temperature must vary according to the initial Me_2SO concentration (Table 1): the higher the concentration, the lower the seeding temperature (T_s). The temperature of the seeding for each concentration was calculated experimentally as the highest temperature which permitted the formation of ice at the top of the vial. Finally, the influence of the incubation temperature and time was studied. The equilibration of the tissue samples in the freezing solution should last enough time to ensure the CPA penetration throughout the tissue without inducing cell damage caused by the CPA toxicity. The incubation of the tissue in the freezing vehicle solution is done at the first step of the cooling process and consists of 15 min at 0 °C in the control group. This control incubation process was compared to exposure at room temperature for 10 min and then 5 more min at 0 °C.

Similarly to our control group, in the six treatments, one ovarian tissue fragment was put in a cryovial containing the freezing solution, which was then loaded in the Bio-Cool. After the cryovial was cooled down to −40 °C, the fast cooling (20 °C/min) until −150 °C was performed by exposing the cryovial to liquid nitrogen vapors. The samples were quenched and stored in the

Table 1
Variation of the different parameters for the optimization of the controlled rate slow cooling protocol.

Parameters	Control	Volume 0.8 mL	CR 0.1 °C/min	CR 1 °C/min	5% v/v Me_2SO	20% v/v Me_2SO	Incubation RT 10 min
Volume	1.8 mL	0.8 mL	1.8 mL	1.8 mL	1.8 mL	1.8 mL	1.8 mL
Cooling rate ([a]T_s to −40 °C)	0.3 °C/min	0.3 °C/min	0.1 °C/min	1 °C/min	0.3 °C/min	0.3 °C/min	0.3 °C/min
[Me_2SO] (% v/v)	10 % v/v	10% v/v	10% v/v	10% v/v	5% v/v	20% v/v	10% v/v
[a]T_s	−5.5 °C	−5.5 °C	−5.5 °C	−5.5 °C	−3 °C	−9 °C	−5.5 °C
[b]Incubation	0 °C 15 min	0 °C 15 min	0 °C 15 min	0 °C 15 min	0 °C 15 min	0 °C 15 min	RT 10 min 0 °C 5min

[a] T_s: temperature of the manual ice seeding.
[b] Incubation refers to the first stage of the controlled rate slow cooling protocol, before the ice seeding.

liquid nitrogen tank.

2.4. CT imaging

The assessment of the CPA concentration inside the frozen tissue samples was determined with the NanoCT device (Bioscan NanoCT®, USA; currently Mediso, Hungary), located at the Centro Nacional de Aceleradores (CNA, Spain). The X-ray attenuation was proved to be proportional to the Me_2SO concentration, as it was published by our group [20]. All images were acquired under the following parameters: a current of 106 mA for a voltage of 75 kV, 500 ms of exposition time per projection and 360 projections per rotation. Each image required a total acquisition time of 3 min. The images were reconstructed using a cone-beam filtered-back projection algorithm to a spatial resolution of 0.2 mm. In order to avoid the rewarming of the samples, the CT imaging of the cryopreserved tissues was performed below the glass transition temperature (~-140 °C), with a specific cooling equipment described elsewhere [20]. In brief, it consists of nitrogen gas pre-cooled with liquid nitrogen which cools the insulating container in which the cryovial is placed during the measurement. The temperature is monitored by a thermocouple located out of the CT area to scan.

Three different software were used during the image processing: Nucline software was used for acquisition (Mediso, Hungary); IVS Image Processing software for reconstruction (Invicro, USA); and PMOD 3.8 software for analysis (PMOD Technologies LLC, Switzerland).

2.5. Statistical analysis

Student's t-test was used to compare Me_2SO concentrations in tissue samples calculated from the CT images. Values of at least $p < 0.05$ were considered statistically significant.

3. Results

In order to evaluate the CPA concentration and distribution, the frozen tissue samples, always kept at −140 °C, were analyzed by X-ray computed tomography. The PMOD software permits to obtain the average X-ray attenuation within a certain VOI (volume of interest), which dimensions (3x3x1 mm^3 in our case) are chosen by the user. The X-ray attenuation values obtained are expressed in *CT values*, which are arbitrary units proportional to the X-ray absorption coefficients of the samples [23]. Since there is a linear relation between the X-ray attenuation and the Me_2SO concentration [20], before analyzing the tissue, we previously obtained a calibration curve by imaging different concentrations of Me_2SO and performing a linear regression analysis. In this way, the coefficients a and b in:

$$[Me_2SO] = a{*}Att + b$$

were obtained, where $[Me_2SO]$ is the Me_2SO concentration (in % v/v) and Att is the average X-ray attenuation (in *CT values*). The experimental values for the slope a and the y-intercept b of the curve were: $a = 0.423 \pm 0.016$ (in $\frac{\% v/v}{CT\ values}$) and $b = -0.54 \pm 0.03$ (in % v/v), with a regression coefficient $r = 0.9993$.

Fig. 1 shows the CT images of bovine ovarian tissues cryopreserved with the control procedure and the different variations of the protocol. The spatial resolution of all images is 0.2 mm. We used a color scale from PMOD software (cold scale) to visualize the images, in which the lowest attenuation corresponds to a dark blue color and the highest attenuation to an intense red color, passing through green, yellow and orange colors for intermediate attenuation values. The typical structure of extracellular ice formed during the controlled rate slow cooling protocol was observed in all the cryovials of each group, showing a low attenuation (dark blue color). This extracellular ice, which appears in a striped shape as dendritic crystals, brings about a solute rejection. As a result, small islands with very high Me_2SO concentration are formed, especially in the inner part of the vials, showing an intense red color. A 3x3x1 mm^3 pink VOI is located in the tissue. The number and characteristic of tissues used in each variation of the control group are described in Table S1 at the supplementary material.

The quantitative study of the average Me_2SO concentration for bovine ovarian tissue is shown in Table 2. The average Me_2SO concentration obtained in the bovine tissue for the control group is 7.50 ± 0.14 % v/v. Obviously, the distribution of the Me_2SO is not uniform inside the tissue. Therefore, the minimum and maximum Me_2SO within the VOI located inside the tissue region is also given in the table. Moreover, the value of the minimum concentration gives us an idea of the possibility of forming ice in the less concentrated parts of the tissue. The results obtained with the different experimental variations are analyzed following.

3.1. Volume

Fig. 1a shows the CT images obtained when we varied the volume: 1.8 mL (control group), and 0.8 mL, volume of UCL protocol. No apparent differences in the concentration were found between both images. Moreover, according to data of Table 2, when decreasing the volume of the solution to 0.8 mL, the average Me_2SO concentration obtained was 7.8 ± 0.4 % v/v, very similar to that of the control group (7.50 ± 0.14 % v/v).

3.2. Cooling rate

The CT images for the parameter of the cooling rate are shown in Fig. 1b. It is not possible to see any difference from the images, although in the image of the fastest CR (1 °C/min), a less number of 'islands' of high Me_2SO concentration is observed. The quantitative result for each cooling rate is compared in Table 2. There seems to be an increase of the average concentration when slowing down the cooling process to 0.1 °C/min, with a concentration of 9.8 ± 0.8 % v/v Me_2SO ($p = 0.3$). An increase in the concentration under this condition was expected, due to a slower ice growth. Nevertheless, the much longer period of time necessary for cooling down to −40 °C may increase the likelihood of intracellular ice, which could explain the high variability expressed in the range, from 0.5 to 45.5 % v/v Me_2SO. When increasing the cooling rate to 1 °C/min, the average concentration was 8.8 ± 0.8 % v/v Me_2SO, lower than that observed at 0.1 °C/min. In this case, the ice formation is too fast and tissue does not have time enough to be permeated by the cryoprotectant. We also observed a decrease on the average size of the ice crystals as a consequence of this higher CR, with a thickness of 0.29 ± 0.04 mm versus 0.33 ± 0.05 mm in the case of the control group. However, the size of the dendritic crystals was maintained the same in the case of the cooling rate of 0.1 °C/min, with an average thickness of 0.33 ± 0.04 mm.

3.3. Initial Me_2SO concentration

Fig. 1c shows the CT images studying the influence of the initial Me_2SO concentration. Evident differences between the three images are observed, showing a darker blue color for the 5 % v/v Me_2SO concentration, indicating a lower concentration, while a green color appears along the vial in the case of the 20 % v/v Me_2SO concentration, and therefore a higher concentration. This could imply a less likely of ice formation in tissues cryopreserved with the

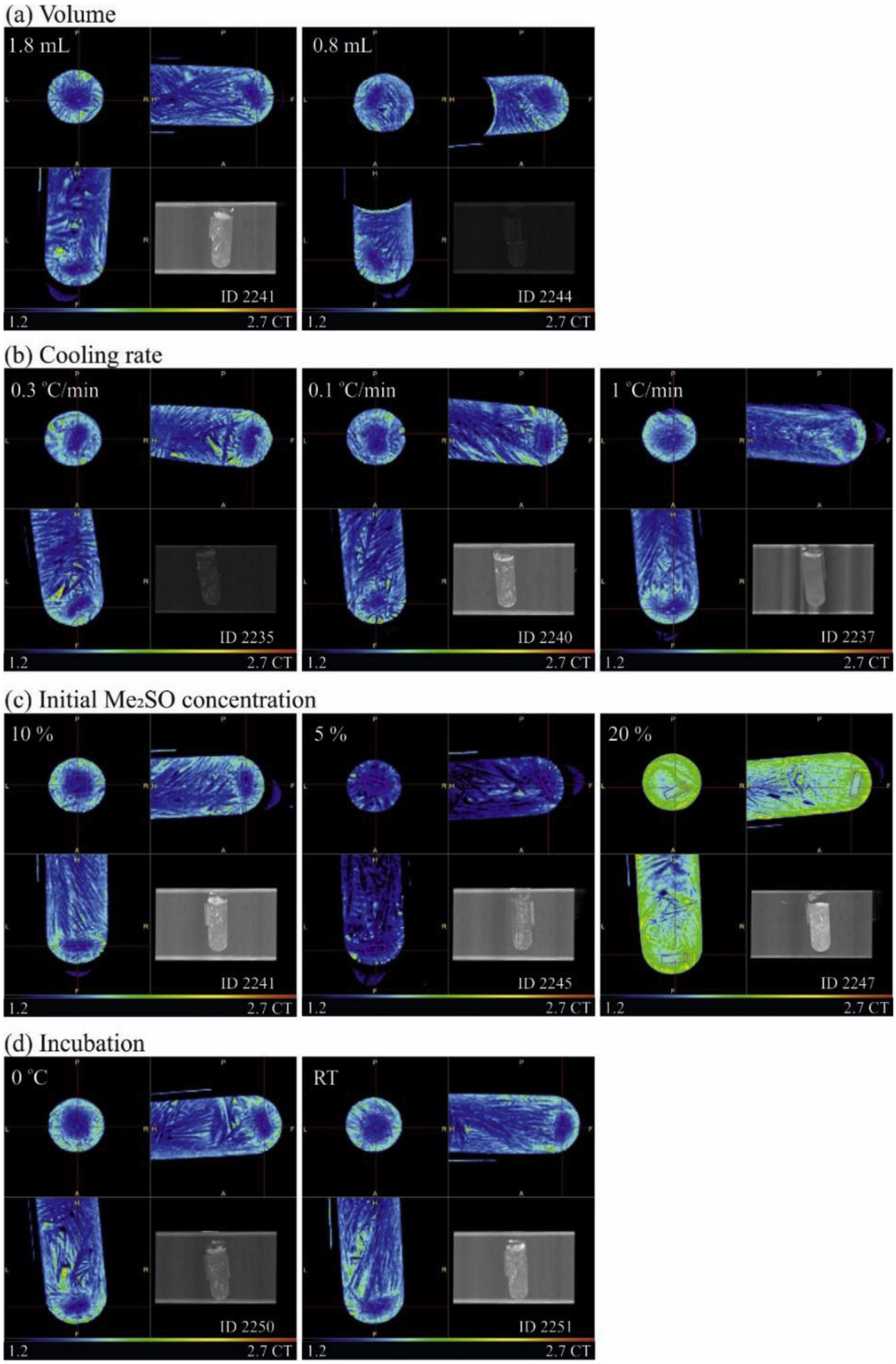

Fig. 1. CT images of bovine ovarian tissues: optimization of a conventional controlled rate slow cooling protocol. Spatial resolution of 0.2 mm. Pink 3x3x1 mm^3 volume of interest (VOI) is located in the tissue. All images are at −140 °C. The parameters of the controlled rate slow cooling protocol varied were: (a) volume (1.8 mL for the control group and

Table 2
Average % v/v Me_2SO data of each sample calculated from a 3x3x1 mm^3 cube within the tissue area. Data presented as average (±standard error) and percentage range (min – max Me_2SO concentration found within the VOI). The Me_2SO concentration is calculated from a calibration curve X-rays attenuation versus % v/v Me_2SO.

Samples	[Me_2SO] (% v/v)	Min – Max [Me_2SO] (% v/v)
Control (n = 6)	7.50 (0.14)	0.32–32.44
Volume 0.8 mL (n = 2)	7.8 (0.4)	1.2–16.3
CR 0.1 °C/min (n = 2)	9.8 (0.8)	0.5–45.5
CR 1 °C/min (n = 2)	8.8 (0.8)	2.0–18.4
5 % v/v Me_2SO (n = 2)	*4.7 (0.3)	0.0–19.2
20 % v/v Me_2SO (n = 2)	*19.8 (1.0)	10.7–38.0
Incubation RT 10 min (n = 2)	*9.4 (0.2)	2.6–24.6

*$p < 0.05$ when compared with the control group.

protocol using a higher Me_2SO concentration. If we analyze the concentration achieved in the tissues using different initial concentrations of Me_2SO, both results differ with the average concentration obtained for the control group ($p < 0.05$). In the case of the lowest concentration used, 5 % v/v Me_2SO, the average concentration obtained was close to the initial value: 4.7 ± 0.3 % v/v Me_2SO. When using 20 % v/v Me_2SO, there is also an increase in the concentration achieved in the tissue (19.8 ± 0.1 % v/v). It is evident that the final Me_2SO concentration achieved in the tissue is determined by the initial concentration of the solution. It must be highlighted that the range of tissue CPA concentrations in this protocol was very homogeneous, with a minimum concentration of 10.7 % v/v Me_2SO, indicating that every part of the tissue was likely permeated with a sufficient CPA concentration to avoid the formation of ice.

3.4. Incubation temperature and time

Fig. 1d shows the impact of the tissue incubation for Me_2SO equilibration. No apparent differences were observed when compared the CT images between these two protocols. Nevertheless, the increase in the temperature of the incubation (room temperature instead of 0 °C) resulted in an increase of the average concentration to 9.4 ± 0.2 % v/v Me_2SO ($p < 0.05$).

4. Discussion

Even though there are more than 100 live births from transplanted ovarian tissue cryopreserved by controlled rate cooling slow, there is evidence of the damage of the follicle population associated with this cryopreservation procedure [1,5]. To better understand the source of this cryodamage, we used bovine ovarian tissue and a CT scan to assess the final Me_2SO concentration achieved in the tissue fragments.

Initially, we tried to reproduce the freezing protocol applied by Dolmans et al. [22], but since we use the Bio-Cool to freeze our samples, the CT images showed that ice formed very fast over the whole cryovial (data not showed). Thus, an adaptation of the freezing protocol was necessary. In such adapted protocol, we observed a lower Me_2SO concentration of 7.5 % v/v Me_2SO compared to 11 % v/v Me_2SO found in human ovarian tissue samples with similar size and frozen with Dolmans et al. [22] protocol (Gallardo et al., unpublished data). This could be due to the different characteristics of the tissues and especially to the different cooling device used (ethanol bath instead of liquid nitrogen based CRF). Nevertheless, in the tissue samples from both species, the CPA distribution in the tissue was clearly not homogeneous and it is true that regions with low concentrations of Me_2SO would be more prone to crystallization.

We then set to determine the influence of four different parameters in the outcome of the controlled rate slow cooling. No statistically significant differences were found when using a lower volume of the solution (0.8 mL vs 1.8 mL). The total volume of the solution influences the time it takes the ice to reach the tissue from the top of the vial, where the seeding is always performed, to the bottom, where the tissue is always located. The dehydration of the tissue and its CPA loading critically depends on this fact. However, this variation in volume does not seem sufficient to observe any difference in the concentration or distribution of Me_2SO within the tissues. The variations of the cooling rate (0.1 °C/min and 1 °C/min vs 0.3 °C/min) did not show significant differences either, although it was observed a lower thickness on the dendritic crystals obtained when the cooling rate was increased to 1 °C/min. The increase of the incubation temperature at room temperature for 10 min followed of a second step at 0 °C for 5 more min, resulted in a significant increase in the Me_2SO concentration when compared with the control protocol (15 min at 0 °C). Nevertheless, the concentration range found in the tissues pointed out to likely ice formation in some parts of it. Furthermore, it is well known that the toxicity of the CPA is increased at higher temperatures [24], which could affect the follicle population and the viability of the tissue after transplantation.

The parameter that mostly influenced permeation seemed to be the initial Me_2SO concentration in the freezing solution, to which the tissue was exposed for 15 min at 0 °C prior to cooling: a significant difference in the final Me_2SO concentration was observed when comparing initial concentrations of 5, 10 and 20 % v/v Me_2SO. An average of 19.8 % v/v Me_2SO was observed in the tissue when using 20 % v/v Me_2SO. Also, the range of CPA concentrations within the tissue, when using 20 % v/v Me_2SO, was very homogeneous, with a minimum of more than 10 % v/v: the grade and homogeneity of the equilibration of the cryoprotectant could avoid ice nucleation thoroughly in the tissue fragment, and may result in improved cryoprotection and a decrease in the damage of the follicle population. A concern of this protocol would again be toxicity resulting of this higher CPA concentration, since it has been reported that Me_2SO concentrations above 10 % v/v could have negative effects on some kind of cells [25]. Nevertheless, any toxic effects might be reduced, considering that the initial incubation time is short and performed at low temperature (0 °C). Then, once cooling has started, the risk of toxicity is furtherly minimized, due to the exponential correlation between CPA toxicity and temperature [24]. For instance, it has been reported that the number of morphologically normal

0.8 mL), (b) cooling rate (0.3 °C/min for the control group, 0.1 °C/min and 1 °C/min), (c) initial Me_2SO concentration (10 % v/v for the control group, 5 % v/v and 20 % v/v) and (d) temperature of incubation (15 min at 0 °C for the control group and 10 min at room temperature followed of 5 min at 0 °C). (For interpretation of the references to color in this figure legend, the reader is referred to the Web version of this article.)

follicles in pieces of zebu ovarian tissue increased when the Me_2SO concentration of the freezing solution was increased to 3M (~21 % v/v) [26]. Another concern about using high Me_2SO concentrations might be the cellular damage produced by the osmotic disruption. Morphological and viability analysis were studied on human ovarian tissue after being cryopreserved by this protocol (20 % v/v Me_2SO). Preliminary tests show no difference when compared with samples cryopreserved by the conventional slow cooling protocols (10 % v/v Me_2SO). This work has been presented on a conference and a manuscript is under preparation [27].

In the light of these results, the following modifications to the control protocol could be implemented to achieve higher Me_2SO concentrations: a volume of 1.8 mL of 20 % v/v Me_2SO vehicle solution, cooling down to −5.5 °C at 2 °C/min with a cooling device based on an alcohol bath (when using a device based on liquid nitrogen cool down to −8 °C), seeding and holding for 15 min, slow cooling down to −40 °C at 0.3 °C/min and fast cooling to −150 °C/min. It is yet to be determined if these adaptations in the protocol will result in improved cryoprotection. Further morphological and viability studies, performing histology and immunological analysis of tissue samples after cryopreservation and transplantation are necessary.

5. Conclusions

The capability of X-ray Computed Tomography to 3D map the concentration of Me_2SO, a widespread cryoprotectant, opens unforeseen possibilities in the field of cryopreservation. 3D mapping process can be done in a wide range of temperatures (from room to cryogenics), as a straightforward consequence, ice crystal and fractures can also be detected by the same strategy. These characteristics constitute an essential tool for the design and optimization of any cryopreservation process, representing a step forward to the challenge of tissue and organ cryopreservation. This technology was used in this work to understand the influence of different parameters of the controlled rate slow cooling protocol for bovine ovarian tissue cryopreservation, giving as result an optimized protocol and a better understanding of the conventional cryopreservation protocol used for ovarian tissue.

The two parameters that showed to have more influence on the final Me_2SO concentration achieved on tissues were the initial concentration of the Me_2SO solution and the temperature and time of the tissue incubation, both showing significant differences with the control groups. For the concrete case of increasing the Me_2SO concentration up to 20 % v/v, apart from achieving a higher average Me_2SO concentration within the tissues, the minimum value of the Me_2SO concentration found was also quite high comparing to the other groups, which might provide a better protection of tissues against the possibility of ice formation.

Conflicts of interest

The author declares no conflict of interest.

Acknowledgements

J. De la Fuente for his assistance in the management of the bovine ovarian tissue. This work has been partially supported by the Junta de Andalucía, Proyectos de Investigación de Excelencia (P08-CTS-03965), Siemens Healthcare S.L.U. (2729/0708) and Retos-Colaboración RTC-2016-4733-1 (MINECO, Spain). C.A. Amorim is Research Associate, FRS - FNRS.

Appendix A. Supplementary data

Supplementary data related to this article can be found at https://doi.org/10.1016/j.theriogenology.2018.06.031.

References

[1] Donnez J, Dolmans MM. Cryopreservation of ovarian tissue: an overview. Minerva Med 2009;100(5):401–13.
[2] Amorim CA, Dolmans MM, David A, Jaeger J, Vanacker J, Camboni A, Van Langendonckt A. Vitrification and xenografting of human ovarian tissue. Fertil Steril 2012;98(5):1291–8.
[3] Amorim CA, Gonçalves PBD, Figueiredo JRD. Cryopreservation of oocytes from pre-antral follicles. Hum Reprod Update 2003;9(2):119–29.
[4] Demirci B, Lornage J, Salle B, Poirel MT, Guerin JF, Franck M. The cryopreservation of ovarian tissue: uses and indications in veterinary medicine. Theriogenology 2003;60(6):999–1010.
[5] Hovatta O. Methods for cryopreservation of human ovarian tissue. Reprod Biomed Online 2005;10(6):729–34.
[6] Jadoul P, Guilmain A, Squifflet J, Luyckx M, Votino R, Wyns C, Dolmans MM. Efficacy of ovarian tissue cryopreservation for fertility preservation: lessons learned from 545 cases. Hum Reprod 2017;32(5):1046–54.
[7] Jensen AK, Macklon KT, Fedder J, Ernst E, Humaidan P, Andersen CY. 86 successful births and 9 ongoing pregnancies worldwide in women transplanted with frozen-thawed ovarian tissue: focus on birth and perinatal outcome in 40 of these children. J Assist Reprod Genet 2017;34(3):325–36.
[8] Donnez J, Dolmans MM, Pellicer A, Diaz-Garcia C, Serrano MS, Schmidt KT, Andersen CY. Restoration of ovarian activity and pregnancy after transplantation of cryopreserved ovarian tissue: a review of 60 cases of reimplantation. Fertil Steril 2013;99(6):1503–13.
[9] Schubert B, Canis M, Darcha C, Artonne C, Smitz J, Grizard G. Follicular growth and estradiol follow-up after subcutaneous xenografting of fresh and cryopreserved human ovarian tissue. Fertil Steril 2008;89(6):1787–94.
[10] Fahy GM, MacFarlane DR, Angell CA, Meryman HT. Vitrification as an approach to cryopreservation. Cryobiology 1984;21(4):407–26.
[11] Pegg DE. Immersion weighing as a method for monitoring the permeation of tissues by cryoprotectants. Cryobiology 2006;53:383.
[12] Pegg DE, Diaper MP. Measurement of permeation of cryoprotectants in tissues by a gravimetric method. Cryobiology 1994;31:571.
[13] Wang RY, Zhang T, Bao Q, Rawson DM. Study on fish embryo responses to the treatment of cryoprotective chemicals using impedance spectroscopy. Eur Biophys J 2006;35:224–30.
[14] Zhang T, Wang RY, Bao QY, Rawson DM. Development of a new rapid measurement technique for fish embryo membrane permeability studies using impedance spectroscopy. Theriogenology 2006;66:982–8.
[15] Fahy GM, Wowk B, Pagotan R, Chang A, Phan J, Thomson B, Phan L. Physical and biological aspects of renal vitrification. Organogenesis 2009;5(3):167–75.
[16] Bidault NP, Hammer BE, Hubel A. Rapid MR imaging of cryoprotectant permeation in an engineered dermal replacement. Cryobiology 2000;40(1):4013–26.
[17] Bischof JC, Mahr B, Choi JH, Behling M, Mewes D. Use of x-ray tomography to map crystalline and amorphous phases in frozen biomaterials. Ann Biomed Eng 2007;35:292–304.
[18] Isbell SA, Fyfe CA, Ammons RL, Pearson B. Measurement of cryoprotective solvent penetration into intact organ tissues using high-field NMR microimaging. Cryobiology 1997;35:165–72.
[19] So PW, Fuller BJ. Hepatic uptake of solutes from the preservation solution during hypothermic storage: a 1H NMR study in rat liver. Cryobiology 2001;42:307–13.
[20] Corral A, Balcerzyk M, Parrado-Gallego Á, Fernández-Gómez I, Lamprea DR, Olmo A, Risco R. Assessment of the cryoprotectant concentration inside a bulky organ for cryopreservation using X-ray computed tomography. Cryobiology 2015;71(3):419–31.
[21] Amorim CA, Rondina D, Rodrigues APR, Gonçalves PBD, de Figueiredo JR, Giorgetti A. Cryopreservation of isolated ovine primordial follicles with propylene glycol and glycerol. Fertil Steril 2004;81(1):735–40.
[22] Dolmans MM, Jadoul P, Gilliaux S, Amorim CA, Luyckx V, Squifflet J, Donnez J, Van Langendonckt A. A review of 15 years of ovarian tissue bank activities. J Assist Reprod Genet 2013;30:305–14.
[23] Adams JE. Quantitative computed tomography. Eur J Radiol 2009;71(3):415–24.
[24] Elmoazzen HY, Poovadan A, Law GK, Elliott JA, McGann LE, Jomha NM. Dimethyl sulfoxide toxicity kinetics in intact articular cartilage. Cell Tissue Bank 2007;8(2):125.
[25] Best BP. Cryoprotectant toxicity: facts, issues, and questions. Rejuvenation Res 2015;18(5):422–36.
[26] Lucci CM, Kacinskis MA, Lopes LHR, Rumpf R, Báo SN. Effect of different cryoprotectants on the structural preservation of follicles in frozen zebu bovine (Bos indicus) ovarian tissue. Theriogenology 2004;61(6):1101–14.
[27] Gallardo M, Paulini F, Corral A, Balcerzyk M, Lucci CM, Merola M, Gallego ALP, Dolmans MM, Risco R, Amorim CA. Utilization of a new freezing protocol containing a higher DMSO concentration to cryopreserve human ovarian tissue. Cryoletters 2018;39(1):80.